

Communication

A General Approach for Generating Fluorescent Probes to Visualize Piconewton Forces at the Cell Surface

Yuan Chang, Zheng Liu, Yun Zhang, Kornelia Galior, Jeffery Yang, and Khalid Salaita

J. Am. Chem. Soc., **Just Accepted Manuscript** • DOI: 10.1021/jacs.5b11602 • Publication Date (Web): 12 Feb 2016

Downloaded from <http://pubs.acs.org> on February 13, 2016

Just Accepted

"Just Accepted" manuscripts have been peer-reviewed and accepted for publication. They are posted online prior to technical editing, formatting for publication and author proofing. The American Chemical Society provides "Just Accepted" as a free service to the research community to expedite the dissemination of scientific material as soon as possible after acceptance. "Just Accepted" manuscripts appear in full in PDF format accompanied by an HTML abstract. "Just Accepted" manuscripts have been fully peer reviewed, but should not be considered the official version of record. They are accessible to all readers and citable by the Digital Object Identifier (DOI®). "Just Accepted" is an optional service offered to authors. Therefore, the "Just Accepted" Web site may not include all articles that will be published in the journal. After a manuscript is technically edited and formatted, it will be removed from the "Just Accepted" Web site and published as an ASAP article. Note that technical editing may introduce minor changes to the manuscript text and/or graphics which could affect content, and all legal disclaimers and ethical guidelines that apply to the journal pertain. ACS cannot be held responsible for errors or consequences arising from the use of information contained in these "Just Accepted" manuscripts.



ACS Publications

GRGDS peptides derived from the fibronectin-III repeat 10 (FN-III₁₀), which primarily bind the $\alpha_5\beta_1$ and $\alpha_v\beta_3$ integrins,¹⁶ 2) the synergy site PHSRN derived from FN-III₉, which is reported to increase cell adhesion when combined with the RGD sequence, 3) the PHSRN(SG)₂RGDS peptide, which includes a spacer between the PHSRN and GRGDS peptides and better mimics the distance between the two binding domains in FN¹⁷ and 4) the SHAVSS and LRAHAVDING peptides, which bind the E-cadherin and N-cadherin receptors, respectively.^{15,18} Standard SPPS protocols were used to generate these α -thioester linear peptides, except for the cRGDfK sequence for which we used a protocol adapted from Xiao et al.¹⁹ Standard NCL conditions were used to couple the peptide to **1** (Figure S4). We subsequently took advantage of the free thiol group inherent to the NCL reaction to site-specifically couple maleimide-modified dyes that take part in FRET with the TAMRA fluorophore, **2**. Typically, we employed Alexa 488 due to its appropriate Forster radius $R_0 = 5.9$ nm with TAMRA (Supplementary Note 1). The molecular probes were then covalently immobilized onto an azide-modified glass slide using standard click reaction conditions. Fluorescence microscopy and FRET analysis showed uniform surface coverage of the tension probes and high quenching efficiency (Figure S5-7). Withholding Cu(II) or using surfaces that lacked the azide did not lead to significant binding of the probe, thus confirming the specificity of the click reaction. The surface density of tension probes ranged from 9000 to 11000 probes/ μm^2 , as determined by quantitative fluorescence imaging (Figure S8).²⁰

To maximize the interaction of the cell receptors with tension probes, we passivated the surface against non-specific binding of cell-generated ECM and serum proteins. Typically, PEG polymers are used for passivation²¹. However, we found that employing PEG polymers for passivation increased background signal and diminished sensitivity (Figure 1). To solve this problem, we tested the zwitterionic silane (3-(dimethyl-(3-(trimethoxysilyl)propyl)ammonio) propane-1-sulfonate), (SBS) (Figure S5),²² and compared its efficiency of passivation against that of PEG polymers (Mw = 2000, 5000 Da).²³ SBS provided enhanced passivation against cell adhesion in comparison to PEG polymers (Figure 1a-1b). Given the importance of the molecular extension of the tension probes, we next aimed to estimate the mean inter-fluorophore distance when the surface was PEG passivated rather than SBS passivated. This was achieved by measuring the FRET efficiency using a TAMRA-PEG₂₄-fluorescein probe and reporting the acceptor-normalized donor intensity (Figure S9). The donor-acceptor distance was greater for the PEG2000 and PEG5000 surfaces in comparison to the SBS passivated surface (Figure 1c). The mean inter-fluorophore distance for SBS surfaces was approximately 2.6 nm, which is in agreement with the predicted 2.4 nm distance based on the Flory model. The TAMRA-fluorescein distance increases by ~ 1 nm when the surface is passivated using PEG5000, which leads to a $\sim 15\%$ decrease in quenching efficiency. These results indicate that the PEG polymer passivation (~ 2000 Da and ~ 5000 Da) leads to molecular crowding of the tension probe, thus placing it in a more extended conformation compared to the samples prepared with SBS passivation. The extension of the tension probe upon passivation with PEG polymers is consistent with the literature showing that polymers with fixed grafting density and increasing molecular weight tend to increase crowding and the transition of polymers to more

brush-like conformations.^{24,25} In contrast, the 1.3 nm length of the SBS was insufficient to crowd the tension probes (Figure 1d). Therefore, SBS provides superior passivation against biofouling and concurrently improves probe sensitivity by reducing background signal. SBS passivation was used in all subsequent cell studies. This result represents the first demonstration of using SBS for cell culture, outperforming PEG polymers, the most widely used reagent for passivation against biofouling.

To test the cRGDfK tension probe, NIH 3T3 cells were

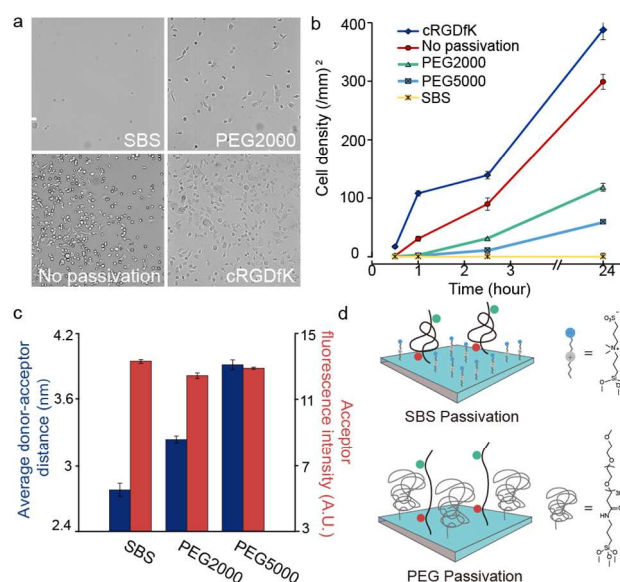


Figure 1. Role of passivation in MTFM probe conformation. (a) Representative brightfield images of NIH 3T3 cells plated for 2.5 hrs on SBS, PEG2000, bare glass, and cRGDfK substrates. Scale bar = 100 μm . (b) Plot showing average cell density on cRGDfK, bare glass, PEG2000, PEG5000, and SBS substrates as a function of time (24 hrs). Error bars represent the standard error of the mean (SEM) of $n = 3$ substrates where a total of 10 regions of interest were averaged from these samples. (c) Bar graph showing the average extension (left y-axis) and acceptor intensity (right y-axis) of MTFM probes as a function of passivation. Error bars represent the SEM of $n = 3$ substrates, where a total of 10 regions were imaged. (d) Model showing the influence of passivation molecule on crowding and extension of tension probes.

plated onto TAMRA-QSY9 sensor modified surfaces for 1 hr to allow the cells to adhere. We used epifluorescence microscopy to image the live cell tension response and reflection interference contrast microscopy (RICM) to monitor cell-substrate binding. A dynamic increase in fluorescence in the tension channel (TAMRA) was observed in regions associated with the cell-binding pattern in RICM (Figure 2a and Movie S1). Tension signal colocalized with GFP-tagged β_3 integrin, confirming that tension signal is integrin mediated (Figure S10, 11). The spatial distribution of tension was relatively dynamic, changing on a time scale of tens of minutes (Figure S12a). We used the worm-like chain (WLC) model and the measured quenching efficiency to estimate the average tension per integrin ligand (Figure 2a and Supplementary Note 2-3). Tension signal dissipated upon treating cells with latrunculin B (latB), an actin polymerization inhibitor, indicating that the signal can be reduced by inhibiting the cellular cytoskeleton (Figure S12b and Movie S2). Taken together, the dynamic fluctuations in tension signal, live cell dual channel integrin/tension imaging, along with the latB experiment show that the reversible fluorescence response is due to me-

chanical tension exerted by integrin receptors engaged to the MTFM sensor. Given the predicted force-fluorescence curve for the PEG₂₄ probes, we expect that the dynamic range of the probes is limited to ~15 pN; the stiffness of the probes increases drastically as the polymer approaches its contour length (Figure S13). The PEG₄₈-based tension probes performed similarly to the PEG₂₄ probes, confirming the modularity of the synthetic approach. The calculated dynamic range of the PEG₄₈ probes is limited to ~5 pN, which suggests that these are more appropriate for signaling pathways that

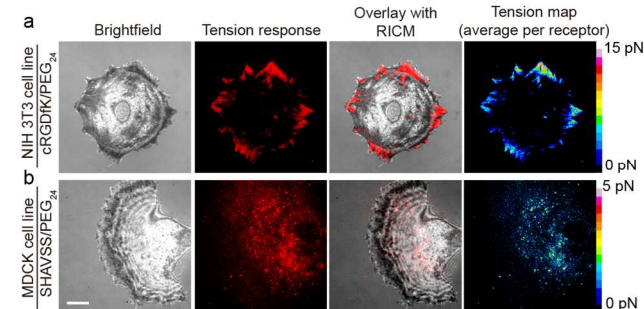


Figure 2. Representative RISM, fluorescence, overlay of fluorescence and RISM, and quantified heat map of tension for cells cultured on the cRGDFK (TAMRA-QSY9) and SHAVSS (TAMRA-Alexa 488) tension probe surfaces. Top row shows an NIH 3T3 cell cultured on the cRGDFK tension probe for 1 hr, while the bottom row shows an MDCK cell cultured on the SHAVSS peptide tension probe for 3 hrs. Raw fluorescence data were converted to a force map. Scale bar = 10 μm .

employ a lower magnitude of tension such as the Notch pathway.^{4,26}

To study the tension generated by E-cadherin receptors, we plated endothelial cells (MDCK) on the SHAVSS peptide tension probes. In contrast to the FA tension patterns observed for the cRGDFK peptide sensor, we observed punctate tension across the cell-substrate junction. The intensity of tension signal was significantly lower for the SHAVSS peptide compared to the cRGDFK peptide. The SHAVSS tension signal was abolished upon treating cells with latB, showing that the signal is generated by the cellular cytoskeleton (Figure S14). Immunostaining for the E-cadherin extracellular domain EC4 displayed puncta at the basal cell surface resembling the signal associated with E-cadherin tension in our assays (Figure S14). We also found that 3T3 fibroblasts did not adhere to the SHAVSS surface, confirming that E-cadherin expression is necessary for cell adhesion. Importantly, tension sensors specific to the N-cadherin ligand, LRAHAVDING, did not yield detectable signal when rat dorsal root ganglion (DRG) neurons were cultured onto substrates (data not shown). Taken together these results indicate that E-cadherin-binding ligands experience lower values of tension than that of integrin ligands, which may reflect the mechanics of cadherin signaling or binding affinity and receptor density differences among these cell types.

To test the capability of the tension probes in long-term imaging, we incubated NIH 3T3 fibroblasts on cRGDFK-Alexa488-TAMRA tension probes. Cells displayed tension patterns at the cell periphery similar to that of the FA markers (Figure 3). After 20 min of incubation, the tension signal became more elongated as cells polarized (Figure 3a). We followed the cRGDFK tension pattern for a period of 64 hrs. During this time, the average tension signal within FAs increased initially and then decreased as cells spread (Figure

3b). Note that the magnitude of integrin tension was correlated with the average size of FAs. As cells fully spread, FAs became slightly smaller in area, and this was accompanied by a decrease in integrin tension. This represents the longest imaging window for mapping receptor-ligand tension using a molecular probe. Minimal change was observed in the fluo-

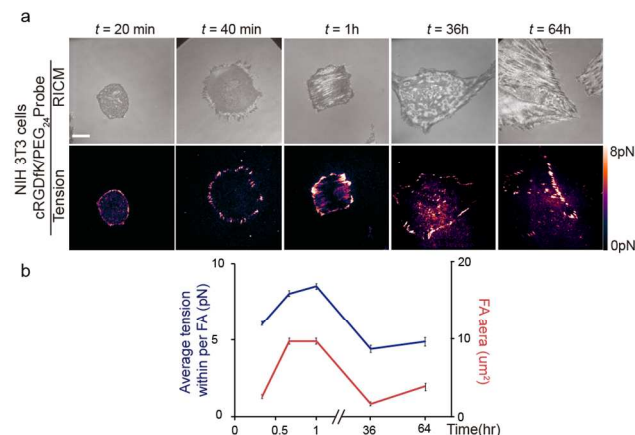


Figure 3. Long-term live cell mechano-imaging using TAMRA-Alexa 488 sensor. (a) RISM and fluorescence images showing the cell-substrate contact zone along with a map of integrin tension at the indicated time points that spanned from 20 min to 64 hrs. Note the changes in cell morphology and force pattern. Scale bar = 10 μm . (b) Plot showing the average tension within FAs (left y-axis), and average FA area (right y-axis) as a function of time over a period of 64 hrs. The error bars represent the SEM from $n=3-4$ cells, where 10-30 FAs were

resence background of both the donor and the acceptor during the 64-hour imaging window (Figure S15).

The peptide PHSRN is found in the FN-III₉, adjacent to the 10th domain that contains the RGD peptide.²⁷ PHSRN has been identified as a synergy ligand that enhances the spreading of cells on the RGD peptide.²⁷⁻³⁰ We asked whether PHSRN carries a mechanical load much like the RGD peptide that supports adhesion. Tension probes with the PHSRN, cRGDFK, PHSRN(SG)₄RGDS and linear GRGDS peptides were immobilized on glass slides. Cells attached and spread inefficiently on PHSRN substrates (Figure 4a). In contrast, cells plated onto surfaces comprised a binary mixture of PHSRN and GRGDS/cRGDFK probes (1:1) spread efficiently. This is in agreement with recent reports showing that PHSRN enhances cell spreading with RGD but is inactive when presented exclusively.^{31,32} The tension signals for cells cultured on PHSRN(SG)₄RGDS, GRGDS and cRGDFK were similar and greater than that of substrates with the binary mixture of GRGDS/cRGDFK and PHSRN (Figure 4b). Note that the samples modified with the binary mixture of RGD ligands and PHSRN display the same total density of MTFM probes but 50% of the RGD ligand density compared to the single component surfaces. Although the affinity of integrins for cRGDFK is greater than that of linear GRGDS, the signals were similar for both ligands, which is in agreement with results obtained using DNA-based tension probes.⁹ We were not able to detect tension signals on the substrates presenting PHSRN exclusively. These data indicate that mechanical tension is not transmitted through the PHSRN synergy ligand, rather its role is most likely in enhancing integrin-ligand affinity. This conclusion clarifies a long-standing question regarding the mechanical role of the PHSRN ligand in cell adhesion. We expect that MTFM probes generated using this modular approach will help elucidate the role of various

ECM components in mediating mechanotransduction processes. A general caveat of this approach is that the dynamic range of the sensor is limited to ~15 pN; thus, while we are

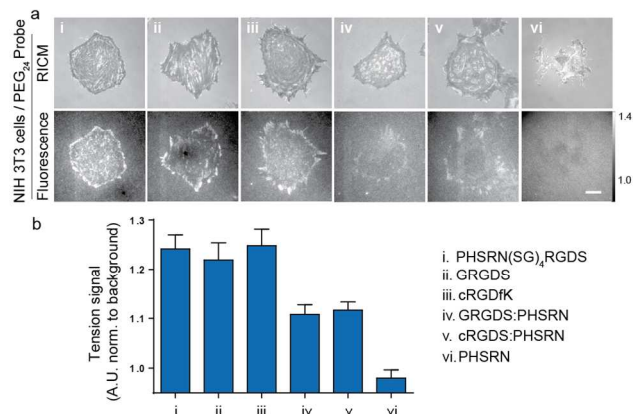


Figure 4. The role of RGD and PHSRN peptides in mediating integrin tension. a) Representative RCM and fluorescence tension images of 3T3 fibroblasts cultured onto PHSRN(SG)₄RGDS, GRGDS, cRGDfK, 1:1 GRGDS: PHSRN, 1:1 cRGDfK: PHSRN, and PHSRN MTFM probes (TAMRA-Alexa 488). Scale bar = 10 μm and contrasts are set identically. b) Bar graph showing the average tension normalized to the background for cells cultured onto the above substrates (a). Data obtained in triplicate from $n=8$ cells in each category for a total of 40 cells, where 10-30 FAs were analyzed from each cell. Note that the average tension for the PHSRN probe was ~2% below the background signal likely due to optical effects from cell adhesion

able to detect differences in the ensemble average tension signal, receptor forces that are $\gg 15$ pN are not distinguishable from lower magnitude signals. Therefore, the lack of statistical difference in tension signal between the GRGDS, cRGDfK, and PHSRN(SG)₄RGDS probes may be due to probe sensitivity rather than the lack of biophysical difference.

In summary, we demonstrated that the integration of SPPS and NCL for MTFM synthesis provides a general and modular approach overcoming stability issues and providing improved sensitivity over previous strategies for tension probe design. This probe can be used to image receptor-ligand forces for peptides amenable to the NCL reaction, which are generally smaller peptides and proteins. There are also some limitations in the choice of dyes that emit in the near-infrared, as these are not generally compatible with SPPS.

ASSOCIATED CONTENT

Supporting Information

Supporting Information and movies. This material is available free of charge via the Internet at <http://pubs.acs.org>.

AUTHOR INFORMATION

Corresponding Author

k.salaita@emory.edu

Notes

The authors declare no competing financial interests.

ACKNOWLEDGMENT

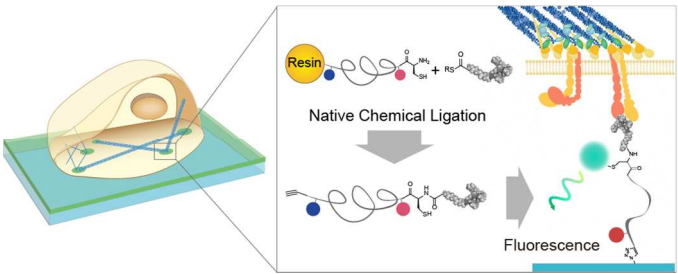
K.S. is grateful for support from the NIH (R01-GM097399), the Alfred P. Sloan Research Fellowship. We also thank Dr. Benjamin Geiger, Department of Molecular Cell Biology at

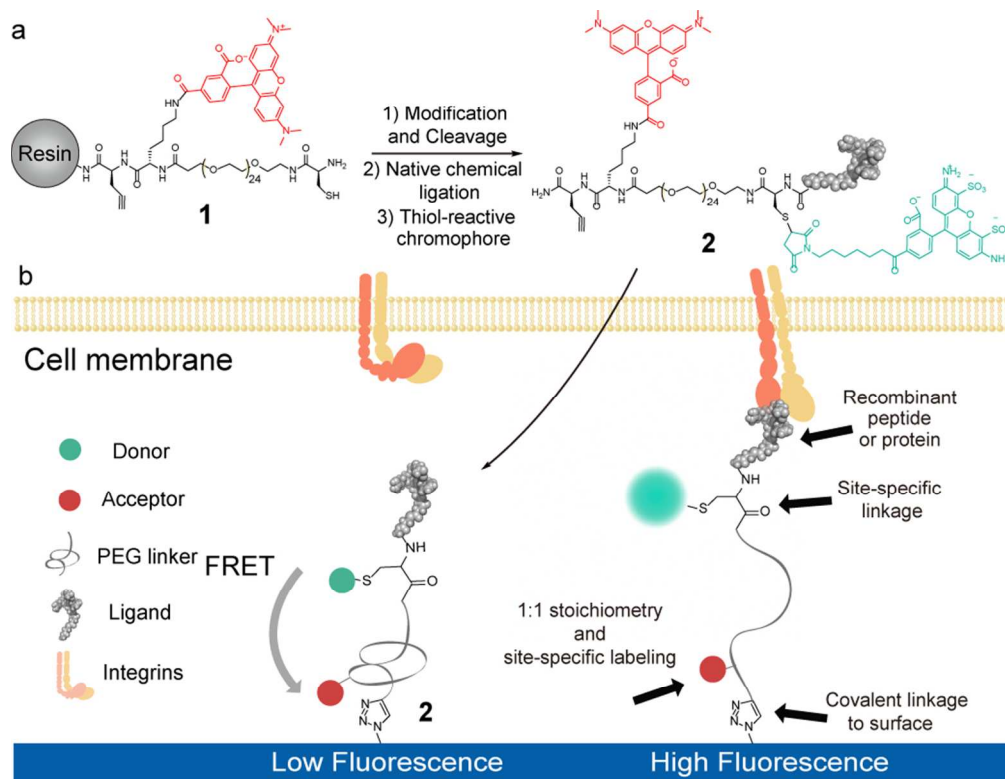
Weizmann Institute, for rat embryonic fibroblast cells transfected with the β_3 -integrin-GFP and David Lynn, Department of Chemistry, Emory University, for solid phase peptide synthesizer.

REFERENCES

- Hynes, R. O. *Cell* **2002**, *110* (6), 673.
- Tan, J. L.; Tien, J.; Pirone, D. M.; Gray, D. S.; Bhadriraju, K.; Chen, C. S. *Proc. Natl. Acad. Sci. U. S. A.* **2003**, *100* (4), 1484.
- Legant, W. R.; Choi, C. K.; Miller, J. S.; Shao, L.; Gao, L.; Betzig, E.; Chen, C. S. *Proc. Natl. Acad. Sci. U. S. A.* **2013**, *110* (3), 881.
- Wang, X.; Ha, T. *Science* **2013**, *340* (6135), 991.
- Borghi, N.; Sorokina, M.; Shcherbakova, O. G.; Weis, W. I.; Pruitt, B. L.; Nelson, W. J.; Dunn, A. R. *Proc. Natl. Acad. Sci. U. S. A.* **2012**, *109* (31), 12568.
- Stabley, D. R.; Jurchenko, C.; Marshall, S. S.; Salaita, K. S. *Nat. Methods* **2012**, *9* (1), 64.
- Liu, Y.; Yehl, K.; Narui, Y.; Salaita, K. J. *Am. Chem. Soc.* **2013**, *135* (14), 5320.
- Jurchenko, C.; Chang, Y.; Narui, Y.; Zhang, Y.; Salaita, K. S. *Biophys. J.* **2014**, *106* (7), 1436.
- Zhang, Y.; Ge, C.; Zhu, C.; Salaita, K. *Nat. Commun.* **2014**, *5*, 5167.
- Liu, Y.; Medda, R.; Liu, Z.; Galior, K.; Yehl, K.; Spatz, J. P.; Cavalcanti-Adam, E. A.; Salaita, K. *Nano Lett.* **2014**, *14* (10), 5539.
- Bhatt, N.; Huang, P. J. J.; Dave, N.; Liu, J. *Langmuir* **2011**, *27*, 6132.
- Mansoor, M. A.; Svandal, A. M.; Ueland, P. M. *Anal. Biochem.* **1992**, *200* (2), 218.
- Blakely, B. L.; Dumelin, C. E.; Trappmann, B.; McGregor, L. M.; Choi, C. K.; Anthony, P. C.; Duesterberg, V. K.; Baker, B. M.; Block, S. M.; Liu, D. R.; Chen, C. S. *Nat. Methods* **2014**, *11* (12), 1229.
- Rajagopalan, P.; Marganski, W. a; Brown, X. Q.; Wong, J. Y. *Biophys. J.* **2004**, *87* (4), 2818.
- Ung, P.; Winkler, Winkler, D. A. *J. Med. Chem.* **2011**, *54* (5), 1.
- Pfaff, M.; Tangemann, K.; Müller, B.; Gurrath, M.; Müller, G.; Kessler, H.; Timpl, R.; Engel, J. *J. Biol. Chem.* **1994**, *269* (32), 20233.
- Craig, J. a.; Rexeisen, E. L.; Mardilovich, A.; Shroff, K.; Kokkoli, E. *Langmuir* **2008**, *24* (18), 10282.
- Noë, V.; Willems, J.; Vandekerckhove, J.; Roy, F. Van; Bruyneel, E.; Mareel, M. J. *Cell Sci.* **1999**, *112*, 127.
- Xiao, J.; Chen, R.; Pawlicki, M. A.; Tolbert, T. J. *J. Am. Chem. Soc.* **2009**, *131* (38), 13616.
- Galush, W. J.; Nye, J. a; Groves, J. T. *Biophys. J.* **2008**, *95* (5), 2512.
- Elbert, D. L.; Hubbell, J. A. *Annu. Rev. Mater. Sci.* **1996**, *26* (1), 365.
- Estephan, Z. G.; Jaber, J. a; Schlenoff, J. B. *Langmuir* **2010**, *26* (22), 16884.
- Jain, a; Liu, R.; Xiang, Y. K.; Ha, T. *Nat. Protoc.* **2012**, *7* (3), 445.
- Backmann, N.; Kappeler, N.; Braun, T.; Huber, F.; Lang, H.-P.; Gerber, C.; Lim, R. Y. H. *Beilstein J. Nanotechnol.* **2010**, *1*, 3.
- De Gennes, P. G. *Macromolecules* **1980**, *13* (19), 1069.
- Kopan, R.; Ilagan, M. X. G. *Cell* **2009**, *137* (2), 216.
- Aota, S.; Nomizu, M.; Yamada, K. M. *J. Biol. Chem.* **1994**, *269* (40), 24756.
- Redick, S. D. *J. Cell Biol.* **2000**, *149* (2), 521.
- Petrie, T. a; Capadona, J. R.; Reyes, C. D.; García, A. J. *Biomaterials* **2006**, *27* (31), 5459.
- Li, F.; Redick, S. D.; Erickson, H. P.; Moy, V. T. *Biophys. J.* **2003**, *84* (2), 1252.
- Feng, Y.; Mrksich, M. *Biochemistry* **2004**, *43* (50), 15811.
- Eisenberg, J. L.; Piper, J. L.; Mrksich, M. *Langmuir* **2009**, *25* (24), 13942.

Insert Table of Contents artwork here





Scheme 1. Synthetic scheme for generating ligand-general molecular tension fluorescence microscopy (MTFM) probes.
87x67mm (300 x 300 DPI)

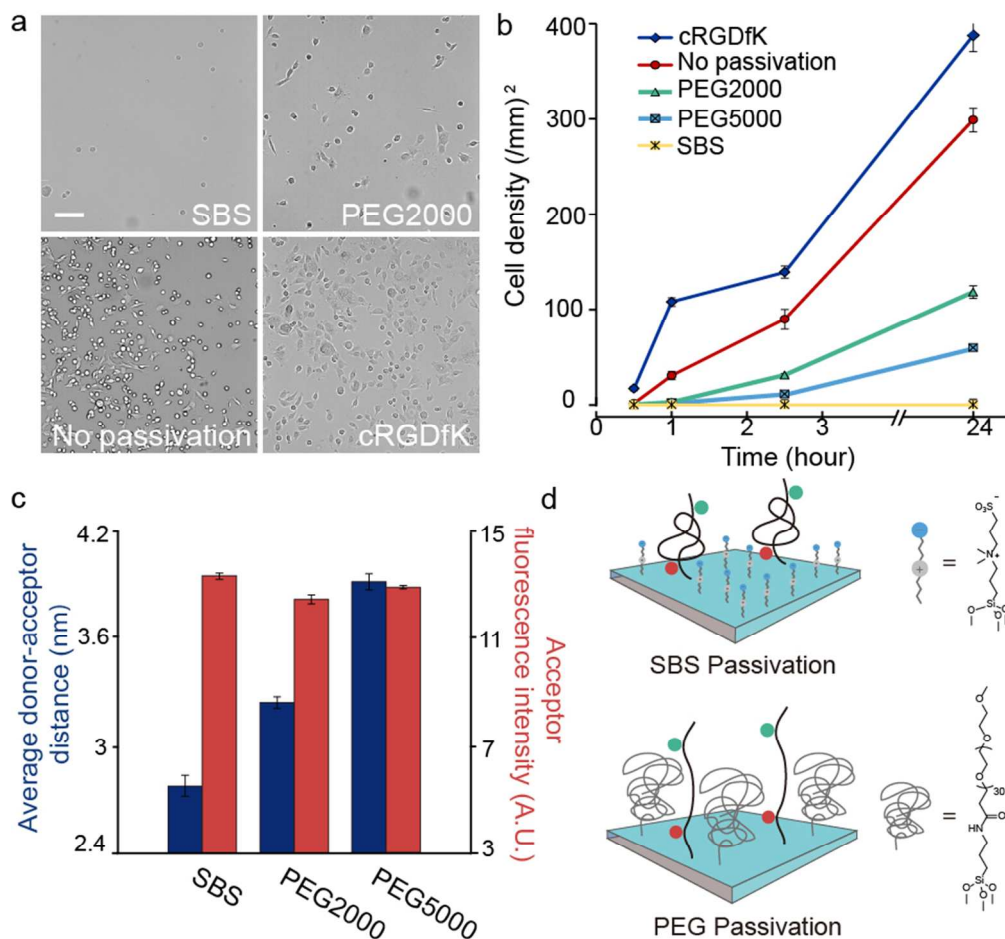


Figure 1. Role of passivation in MTFM probe conformation. (a) Representative brightfield images of NIH 3T3 cells plated for 2.5 hrs on SBS, PEG2000, bare glass, and cRGDfK substrates. Scale bar = 100 μ m. (b) Plot showing average cell density on cRGDfK, bare glass, PEG2000, PEG5000, and SBS substrates as a function of time (24 hrs). Error bars represent the standard error of the mean (SEM) of $n = 3$ substrates where a total of 10 regions of interest were averaged from these samples. (c) Bar graph showing the average extension (left y-axis) and acceptor intensity (right y-axis) of MTFM probes as a function of passivation. Error bars represent the SEM of $n=3$ substrates, where a total of 10 regions were imaged. (d) Model showing the influence of passivation molecule on crowding and extension of tension probes.

81x76mm (300 x 300 DPI)

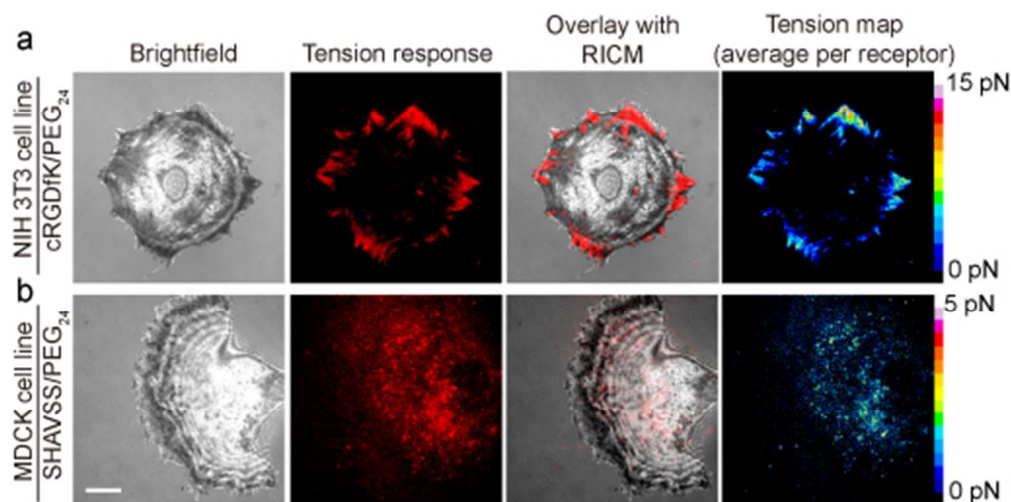


Figure 2. Representative RISM, fluorescence, overlay of fluorescence and RISM, and quantified heat map of tension for cells cultured on the cRGDfK (TAMRA-QSY9) and SHAVSS (TAMRA-Alexa 488) ten-sion probe surfaces. Top row shows an NIH 3T3 cell cultured on the cRGDfK tension probe for 1 hr, while the bottom row shows an MDCK cell cultured on the SHAVSS peptide tension probe for 3 hrs. Raw fluorescence data were converted to a force map. Scale bar = 10 μ m.
87x43mm (150 x 150 DPI)

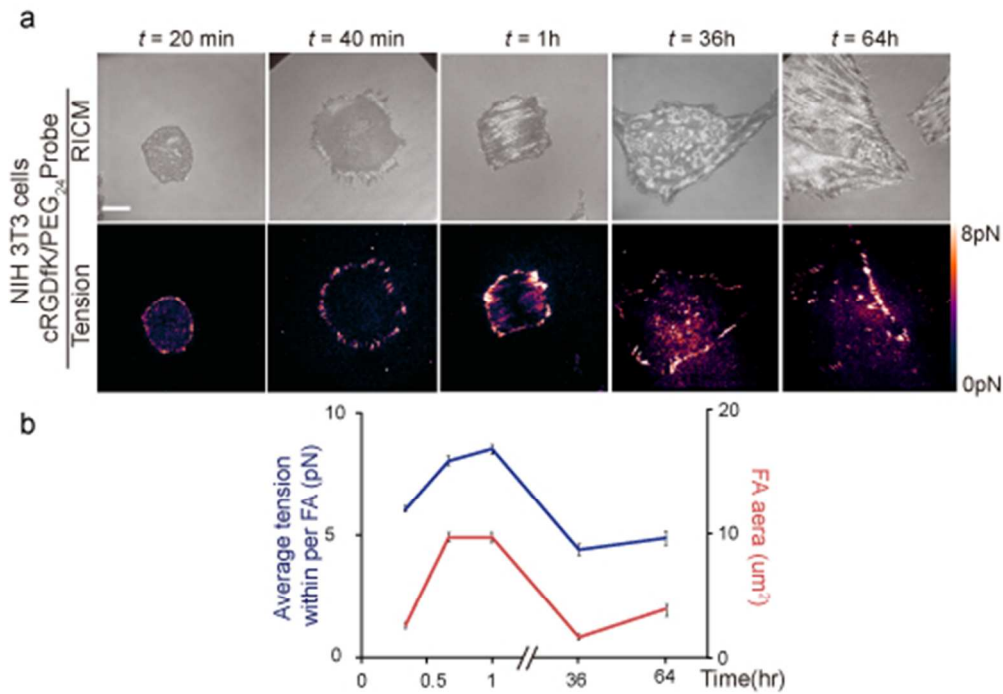


Figure 3. Long-term live cell mechano-imaging using TAMRA-Alexa 488 sensor. (a) RISM and fluorescence images showing the cell-substrate contact zone along with a map of integrin tension at the indicated time points that spanned from 20 min to 64 hrs. Note the changes in cell morphology and force pattern. Scale bar = 10 μm . (b) Plot showing the average tension within FAs (left y-axis), and average FA area (right y-axis) as a function of time over a period of 64 hrs. The error bars represent the SEM from $n=3-4$ cells, where 10-30 FAs were analyzed from each cell.

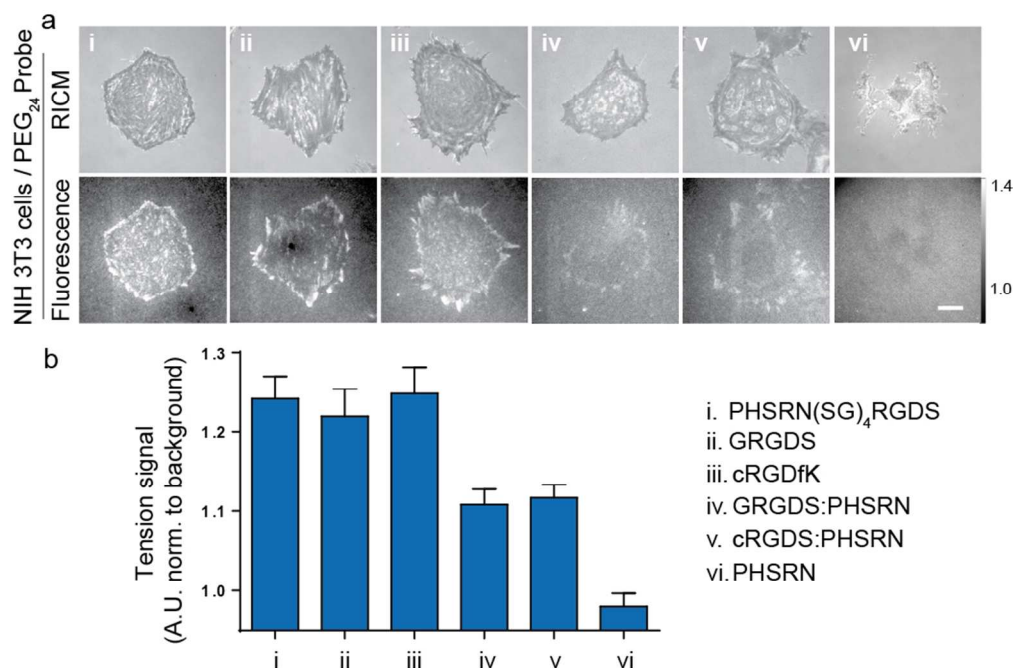
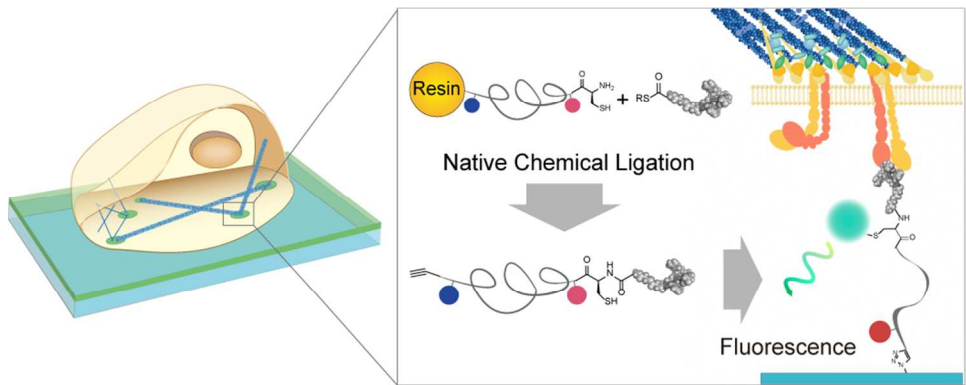


Figure 4. The role of RGD and PHSRN peptides in mediating integrin tension. a) Representative RICM and fluorescence tension images of 3T3 fibroblasts cultured onto PHSRN(SG)₄RGDS, GRGDS, cRGDfK, 1:1 GRGDS: PHSRN, 1:1 cRGDfK: PHSRN, and PHSRN MTFM probes (TAMRA-Alexa 488). Scale bar = 10 μm and contrasts are set identically. b) Bar graph showing the average tension normalized to the background for cells cultured onto the above substrates (a). Data obtained in triplicate from n=8 cells in each category for a total of 40 cells, where 10-30 FAs were analyzed from each cell. Note that the average tension for the PHSRN probe was ~2% below the background signal likely due to optical effects from cell adhesion.

88x59mm (299 x 299 DPI)



TOC
93x35mm (300 x 300 DPI)